The Near-Real-Time SCALE-LETKF System: A Case of the September 2015 Kanto-Tohoku Heavy Rainfall

Guo-Yuan Lien[1], Takemasa Miyoshi[1, 2, 3], Seiya Nishizawa[1], Ryuji Yoshida[1, 4], Hisashi Yashiro[1], Sachiho A. Adachi[1], Tsuyoshi Yamaura[1], and Hirofumi Tomita[1]

[1]*RIKEN Advanced Institute for Computational Science, Kobe, Japan*
[2]*Department of Atmospheric and Oceanic Science, University of Maryland, College Park, Maryland, USA*
[3]*Japan Agency for Marine-Earth Science and Technology (JAMSTEC), Yokohama, Japan*
[4]*Research Center for Urban Safety and Security, Kobe University, Kobe, Japan*

Abstract

With a goal of real-time, high-resolution, short-term prediction of heavy rainfall systems, the SCALE-LETKF was developed implementing the local ensemble transform Kalman filter with the Scalable Computing for Advanced Library and Environment-Regional Model (SCALE-RM). The system has been running in near real time experimentally since May 2015, configured for weather analyses and forecasts at 18-km resolution for a 5760 × 4320 km area around Japan. Among the data for more than one year, the near-real-time forecasts and the 3-km resolution downscaling simulations are demonstrated for a selected case of the September 2015 Kanto-Tohoku heavy rainfall associated with Typhoon Etau (2015). The typhoon track was successfully analyzed and predicted by the system, and the line-shaped rainband producing heavy rainfall can be reasonably forecasted by the downscaling simulation from the near-real-time data.

(**Citation**: Lien, G.-Y., T. Miyoshi, S. Nishizawa, R. Yoshida, H. Yashiro, S. A. Adachi, T. Yamaura, and H. Tomita, 2017: The near-real-time SCALE-LETKF system: A case of the September 2015 Kanto-Tohoku heavy rainfall. *SOLA*, **13**, 1−6, doi:10.2151/sola.2017-001.)

1. Introduction

Data assimilation is a key component in numerical weather prediction (NWP). In the recent 15 years, the ensemble Kalman filter (EnKF; Evensen 1994, 2003), benefited from its flow-dependent error covariance and ease of implementation, has become a popular data assimilation method. It can be used alone or in combination with a 3-dimensional/4-dimensional variational method (3DVar/4DVar) for a hybrid system (e.g., Wang et al. 2013). Recent studies have shown that, in an operational setup, the global NWP systems using the EnKF or hybrid-EnKF/variational data assimilation schemes can perform as well as using the state-of-the-art 4DVar (Buehner et al. 2013; Bonavita et al. 2015).

To accurately simulate high-impact weather phenomena such as heavy convective rainfall systems, running a model at convection-resolving resolution is necessary (Roberts and Lean 2008; Prein et al. 2015). A regional NWP system can be used to increase the model resolution of an area of interest at a relatively low cost. Therefore, regional EnKF systems have also been widely developed and tested (Zhang et al. 2006; Meng and Zhang 2007; Torn and Hakim 2008; Anderson et al. 2009; Miyoshi and Aranami 2006; Miyoshi and Kunii 2012; Kunii 2014), and they have shown promising results in analyzing and predicting a variety of mesoscale phenomena, such as tropical cyclones (e.g., Zhang et al. 2009; Zhang and Weng 2015; Torn 2010) and convective rainstorms (e.g., Yussouf et al. 2013; Kunii 2014; Jones et al. 2015).

As an essential part of the work for the "Big Data Assimilation" (BDA) project described by Miyoshi et al. (2016a, b), we developed the SCALE-LETKF system, implementing the local ensemble transform Kalman filter (LETKF; Hunt et al. 2007) with a regional weather model, the Scalable Computing for Advanced Library and Environment-Regional Model (SCALE-RM). We aim to use this system for the goal of high-resolution real-time NWP using a very large supercomputer (Miyoshi et al. 2016a, b). Meanwhile, we also aim to build a highly configurable regional LETKF data assimilation which can be conveniently used in a wide range of research. There have been a few existing ensemble data assimilation systems available for research use, such as the Data Assimilation Research Testbed (DART; Anderson et al. 2009) and Community Gridpoint Statistical Interpolation (Community GSI; Shao et al. 2015). The distinct foci of the SCALE-LETKF include 1) implementing the LETKF scheme which is not included in DART or Community GSI, 2) providing a data assimilation package for the SCALE-RM, and 3) having been tested on the Japan's flagship supercomputer, the K computer, with over 70,000 nodes during the development, aware of the parallelization efficiency of high performance computing.

This article first introduces the newly developed SCALE-LETKF system (Section 2) and describes the experiment in a low-resolution and near-real-time (NRT) configuration to examine its performance, stability, and computational requirement (Section 3). Next, the analyses and forecasts for a high impact heavy rainfall case, the September 2015 Japan Kanto-Tohoku heavy rainfall associated with Typhoon Etau (2015) is presented in Section 4. Since the present configuration of the NRT SCALE-LETKF is simpler than the state-of-the-art operational systems (e.g., fewer types of observations assimilated), and the newly developed SCALE model may not be as mature as other well-tuned NWP models, the performance of the NRT SCALE-LETKF system would be worse than the operational systems. Instead, this study aims to present the first step toward future expansions including BDA and other possible research applications.

2. The SCALE-LETKF

The SCALE is an open-source basic library for weather and climate simulations. The SCALE-RM, built upon SCALE, is a regional NWP model, with capability of large eddy simulation (LES) when run at very high resolution. The model descriptions are provided by Nishizawa et al. (2015) and Sato et al. (2015), and the source code and documents of SCALE and SCALE-RM are available at http://scale.aics.riken.jp/ .

In this study, we run SCALE-RM at relatively low resolution (18 km and 3 km). Moist physical process is parameterized by a 6-class single-moment bulk microphysics scheme (Tomita 2008). No cumulus parameterization is used, simply because no cumulus parameterization scheme has yet been implemented into the SCALE model. Radiation is computed by the mstrnX scheme (Sekiguchi and Nakajima 2008). Turbulence is computed by the Mellor-Yamada Nakanishi-Niino Level 2.5 scheme (Mellor and

Corresponding author: Guo-Yuan Lien, Data Assimilation Research Team, RIKEN Advanced Institute for Computational Science, 7-1-26, Minatojima-minami-machi, Chuo-ku, Kobe, Hyogo 650-0047, Japan. E-mail: guo-yuan.lien@riken.jp.

Yamada 1982; Nakanishi and Niino 2004). Land surface processes are parameterized by a bulk surface model (Beljaars and Holtslag 1991; Wilson 2001) and a simple single-layer urban canopy model (Kusaka et al. 2001). Sea surface temperature is assumed to be constant given by the initial condition.

The LETKF (Hunt et al. 2007) is a variant of the EnKF data assimilation schemes. It has been widely used with a variety of geophysical models [e.g., Szunyogh et al. (2008) and Miyoshi et al. (2010) for global models, Miyoshi and Aranami (2006) and Miyoshi and Kunii (2012) for regional models]. It is shown to be suitable for parallel computing because it performs analysis independently for each grid with a subset of observations (Miyoshi and Yamane 2007). We have developed the SCALE-LETKF by coupling the LETKF with the SCALE-RM; besides, we take advantage of the experiences gained from past implementations with other models (e.g., Miyoshi and Kunii 2012; Kunii 2014; Yashiro et al. 2016) to make it a highly configurable (Supplement 1) and computationally scalable data assimilation package for regional NWP, aiming for the capability of NRT weather analyses and forecasts at high resolution. We have made the SCALE-LETKF code available at https://github.com/takemasa-miyoshi/letkf, integrated with the LETKF applications to other models.

3. The near-real-time SCALE-LETKF application

We set up the NRT SCALE-LETKF to conduct 6-hourly data assimilation cycles over a 5760 × 4320 km domain centered at Japan (Fig. 1). It assimilates the conventional observation data used for the U.S. National Centers for Environmental Prediction (NCEP) operational system (i.e., NCEP PREPBUFR), including upper-air and surface in-situ observations and satellite derived data such as satellite winds, but excluding radiance data. The NCEP PREPBUFR data are provided in a NRT basis (delay time shown in Fig. 2) on the National Oceanic and Atmospheric Administration (NOAA)'s National Operational Model Archive and Distribution System (NOMADS; http://nomads.ncep.noaa.gov/). The horizontal grid spacing of the SCALE-RM is 18 km (320 × 240 grids), and there are 36 terrain following vertical levels from the surface to about 29 km. The ensemble size is 50. In a data assimilation cycle, 9-h ensemble forecasts at the original 18-km resolution are conducted to evolve the error covariance for the 4D-LETKF (Hunt et al. 2004), assimilating observations within the 3 to 9-h forecast window. The lateral boundary conditions for the first 6-h ensemble forecasts in the data assimilation cycle are from the NCEP Global Forecast System (GFS) 0.5° operational analyses[1], where the same data are applied to all members. Besides, after the analysis, a single 120-h deterministic forecast is conducted from the ensemble mean in every 6-h cycle, for which the lateral boundary conditions are from the GFS 0.5° operational deterministic forecasts. We have also downloaded the GFS model data from the NOAA NOMADS.

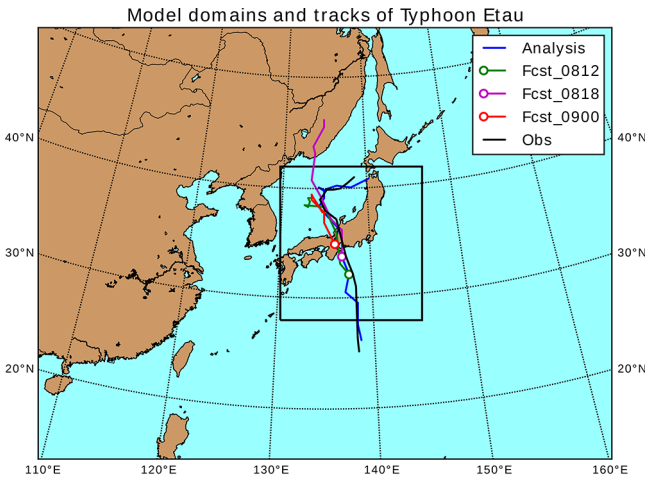

Fig. 1. The model domain of the NRT SCALE-LETKF. Also shown are the tracks of Typhoon Etau in the NRT SCALE-LETKF analysis (blue line), the JMA best-track observation (black line), and the 48-h SCALE-RM forecasts from three cycles (1200 UTC 8 September: green; 1800 UTC 8 September: magenta; 0000 UTC 9 September: red lines), with circles indicating their initial times. The domain of the 3-km resolution downscaling forecasts is shown in black rectangle.

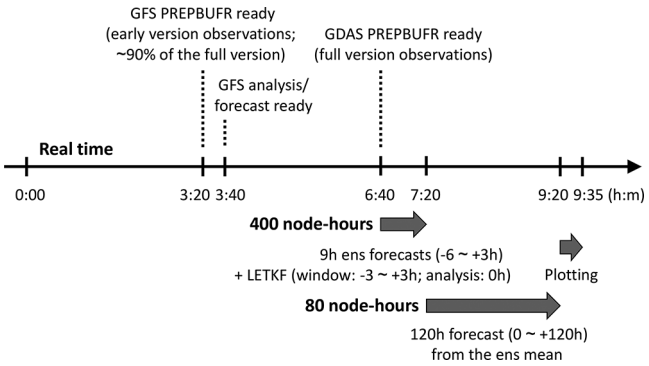

Fig. 2. The computational timeline of one DA cycle in the NRT SCALE-LETKF. All time expressions are relative to the analysis time in the cycle. The thick time coordinate in the middle indicates the real-world time; other time expressions represent the model time. It assumes no queuing time on the K computer.

The state variables analyzed in the NRT SCALE-LETKF include the horizontal and vertical wind components, temperature, pressure, and mixing ratios of water vapor, cloud water, could ice, rain, snow, and graupel. The upper-level mixing ratios above 11 km are not updated. Sea surface temperature is not analyzed by the system but the one in the NCEP GFS analysis is directly used in each cycle. Covariance inflation is applied by a combination of multiplicative inflation and relaxation to prior perturbation (Zhang et al. 2004) schemes. The background error covariance is first multiplicatively inflated by a constant factor of 2.0. In addition, the analysis perturbation is relaxed to the background perturbation with a weight of 0.8 for the background and 0.2 for the analysis. This helps consider the inhomogeneous observation coverage. The two-step inflation considerably inflates the covariance to compensate for the detrimental effect of the fixed boundary data (Torn et al. 2006; Miyoshi and Kunii 2012). The length scales of the covariance localization are horizontally 400 km and vertically 0.3 in the natural logarithmic pressure coordinate.

Figure 2 shows the computational timeline of the NRT SCALE-LETKF system, assuming no job queuing time. The main computation (i.e., the data assimilation cycle and the deterministic forecast) is performed on the K computer using about 400 and 80 node-hours[2], respectively, while the other data pre-processing, post-processing, and visualization tasks are performed in an independent Linux server. Therefore, the NRT SCALE-LETKF takes about 60,000 node-hours per month, or about 0.1% of the total capacity of the K computer. In the current configuration, we use the full version observations from the NCEP Global Data Assimilation System (GDAS), so that in each cycle the computation starts about 6.6 hours in the real-world time after the model analysis time. The 120-h forecast product could be available in the next 3 hours (i.e., about 10 hour lag to the real-world analysis time) using a smaller number of computing nodes. The early version (GFS) observations can be instead used for more timely results (i.e., about 3 hours in advance to the current schedule).

We initiated the current NRT SCALE-LETKF at 0000 UTC 7 May 2015 by arbitrarily choosing a series of GFS analyses at

[1] The NCEP GFS analysis and forecast are performed at higher resolution (semi-Lagrangian T1534) but we used its 0.5° resolution product to drive the NRT SCALE-LETKF analysis and forecast.

[2] The number of nodes used for the computation job times the execution time in hours.

different dates in a similar season in 2013 and 2014. The data assimilation has been cycled continuously, and 120-h forecasts have been conducted every 6 hours until now for more than one year. Verified with the 0.5° NCEP GFS analyses, Fig. 3 shows the one-year evolution of the horizontally domain-averaged root-mean-square (RMS) differences and biases of the analysis temperature, and Fig. 4 shows the RMS differences (solid lines) and mean biases (dashed lines) of the 500-hPa temperature, 500-hPa U-wind, and 700-hPa relative humidity in the 120-h deterministic forecasts initialized from the analysis ensemble means, versus forecast times, averaged within the same period.

These results indicate that the LETKF data assimilation has functioned well: It has run stably and has maintained roughly constant RMS differences and low biases in the analysis (Fig. 3), and the errors (RMS differences) grow with forecast time (Fig. 4). We note that although the NCEP GFS analyses and forecasts are used as the boundary conditions for the NRT SCALE-LETKF system, the domain-average differences from the GFS analyses can still grow by more than twice in wind and temperature fields in the 120-h forecasts, due to the sufficiently large model domain. This implies that the low errors in the NRT SCALE-LETKF analyses would not be achieved if the LETKF were not properly functioned, even with the GFS boundaries. Some more verification results and related discussion are provided in Supplement 2.

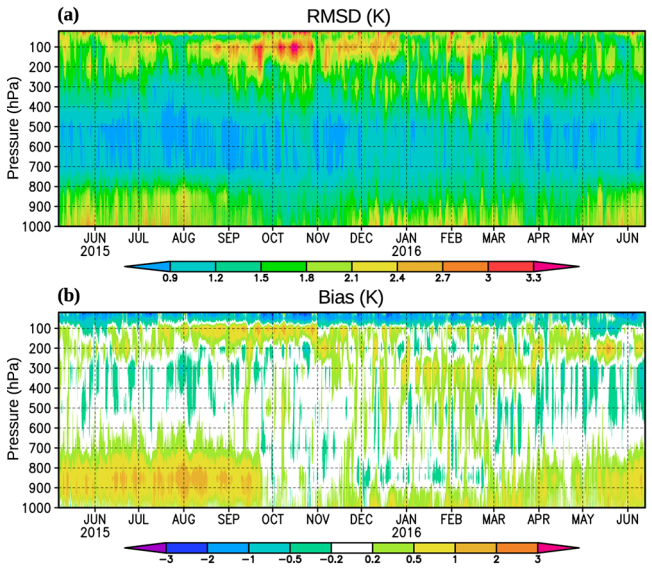

Fig. 3. Time evolution of the horizontal (a) root-mean-square differences and (b) mean biases of temperature (K) in SCALE-LETKF analyses versus model height, verified against the 0.5° GFS analysis during the period from 7 May 2015 to 13 June 2016.

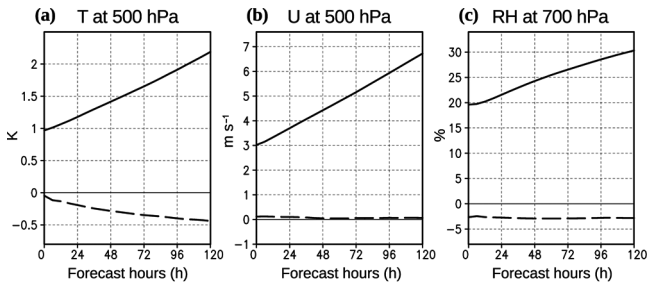

Fig. 4. Root-mean-square (RMS) differences (solid lines) and mean biases (dashed lines) of (a) 500-hPa temperature (K), (b) 500-hPa U-wind (m s^{-1}), and (c) 700-hPa relative humidity (%) in the SCALE-LETKF 120-h deterministic forecasts versus forecast times, verified against the 0.5° GFS analysis, and averaged within the period from 7 May 2015 to 13 June 2016.

4. A heavy rainfall case study: Typhoon Etau

Typhoon Etau (2015) was generated at 1200 UTC 7 September 2015 over the Pacific Ocean south to Japan, and it quickly moved northward and made landfall in Aichi Prefecture, Japan at about 0100 UTC 9 September. The typhoon had never been a strong typhoon during its short lifetime. The maximum intensity reached 985 hPa in central sea level pressure based on the Japan Meteorological Agency (JMA) best track data. It caused limited damage around the landfall area but extensive damage over the remote Kanto-Tohoku region by the induced record-breaking heavy rainfall. The heavy rainfall mainly came from a north-south oriented line-shaped rainband about 500 km eastward to the typhoon center (Figs. 5f and 5i). The maximum 24-h accumulated rainfall exceeded 550 mm in Tochigi Prefecture, which caused severe flooding over the Kinugawa river basin.

4.1 Analyses and forecasts from the near-real-time system

The track of Typhoon Etau in the 18-km resolution NRT SCALE-LETKF analysis from 1200 UTC 7 September to 1200 UTC 11 September 2015 (i.e., part of the year-long continuous cycling experiment) is shown in the blue line in Fig. 1. The central location of the simulated typhoon is defined based on the maximum vorticity at 700 hPa, which identifies the central location more stably even after the typhoon quickly weakened to a tropical storm by making landfall; Figure 1 includes the track in the post-typhoon period. Although we did not explicitly provide the typhoon center information to the data assimilation system, the analyzed typhoon track agreed generally well with the JMA best track (black line in Fig. 1). As for the typhoon intensity, the minimum central sea level pressure in the NRT SCALE-LETKF analysis was 996 hPa, reached prior to the landfall, but weaker than the JMA best-track data (985 hPa), which may be partly because data assimilation with only the conventional data would not be good enough to spin up the typhoon to the observed intensity within its short lifetime of about 1.5 days before landfall (Fig. S3-1 in Supplement 3).

The NRT SCALE-LETKF runs 5-day forecasts from the ensemble mean in every 6-h cycle. In Fig. 1, we also show the first 48-h forecast tracks from 3 consecutive cycles, 1200 UTC 8 September (Fcst_0812, green), 1800 UTC 8 September (Fcst_0818, magenta), and 0000 UTC 9 September (Fcst_0900, red). The track forecasts reasonably agree with the best track data in the early forecast times and lead to similar landfall locations, but they diverge in the later forecast times, partly due to the weakness of the typhoon in the later period when the center locations are not well defined. The intensity forecasts agree that the typhoon is relatively weak at the time of landfall (Fig. S3-1 in Supplement 3).

The 1-h accumulated precipitation of the 0000 UTC 9 September forecast is shown in Figs. 5a, 5d, and 5g, corresponding to 3, 24, and 48 hour lead times, respectively. Compared to the JMA radar-based precipitation estimates (Figs. 5c, 5f, and 5i), we see a good correspondence of the rainband location and patterns in the 3-h short-term forecast (Figs. 5a and 5c), indicating that the NRT SCALE-LETKF successfully captures the typhoon location and structure by using only the conventional observation data. However, the 18-km resolution is not sufficient to resolve the fine structure of the typhoon, and the absence of a cumulus parameterization, which is generally required at the 18-km resolution (Prein et al. 2015), may also degrade the results. It is seen in the longer forecasts (Figs. 5d and 5g) that the line-shaped heavy rainband in the Kanto-Tohoku region around 140°E appears only vaguely in the NRT SCALE-LETKF forecast, and the forecast precipitation is unrealistically confined in scattered convective cells mainly because the model without a cumulus parameterization cannot produce the sub-grid-scale precipitation.

4.2 Offline downscaling forecasts

The above 18-km results were directly obtained from the NRT SCALE-LETKF system in near real time. Since the benefits of the

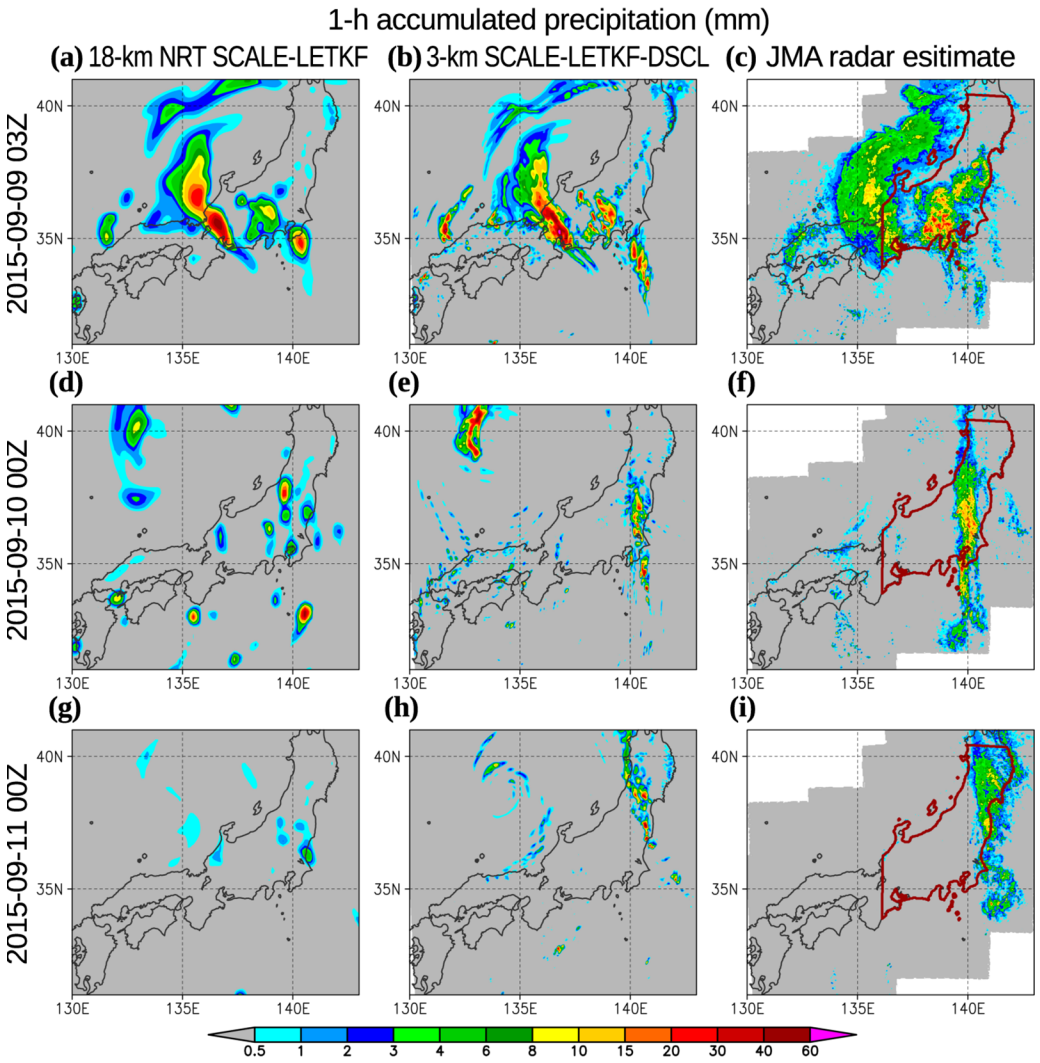

Fig. 5. The previous-1-h accumulated precipitation (mm) at (a)–(c) 0300 UTC 9 September (3-h forecasts), (d)–(f) 0000 UTC 10 September (24-h forecasts), and (g)–(i) 0000 UTC 11 September 2015 (48-h forecasts) in (a), (d), (g) the 18-km resolution NRT SCALE-LETKF forecast and (b), (e), (h) the 3-km resolution downscaling forecast (SCALE-LETKF-DSCL), both initialized at 00:00 UTC 9 September, and (c), (f), (i) the JMA radar based precipitation estimate. White areas mean no data. The land area enclosed by the thick red contour indicates the verification area for threat score calculation.

regional data assimilation system are mostly on the small scale prediction in a shorter time range, we additionally conduct 3-km resolution downscaling forecasts for 48 hours from 3 initial times (1200 UTC and 1800 UTC 8 September, and 0000 UTC 9 September) in a smaller domain shown in the black rectangle in Fig. 1, using the offline nesting function in the SCALE-RM (hereafter SCALE-LETKF-DSCL). Namely, the initial conditions for the inner 3-km resolution domain are interpolated from the 18-km resolution NRT SCALE-LETKF analyses, and the boundary conditions come from the 18-km resolution model forecasts, which were already shown before. We note that it is more reasonable not to use a cumulus parameterization at the 3-km resolution. The 3-km precipitation forecast from 0000 UTC 9 September (Figs. 5b, 5e, and 5h) shows a better fine structure, and importantly the north-south oriented line-shaped rainband located in the Kanto-Tohoku region. It matches well with the observed rainband, although the scale of the simulated rainband is smaller, and its intensity is weaker than that in the observation.

To objectively evaluate the 3-km resolution precipitation forecasts, we calculate their threat scores (TS) verified against the 1-km JMA radar based precipitation estimates over the land-only area shown by the thick red contour in Figs. 5c, 5f, and 5i, where the heavy rainfall occurred. The TS is defined as:

$$\mathrm{TS} = \frac{H}{F + O - H} \tag{1}$$

where F is the area where the forecasted precipitation exceeds a given threshold, O is the area where the observed precipitation exceeds the threshold, and H is the area that both the forecasted and observed precipitation exceeds the threshold, meaning a successful prediction. The TS ranges from 0 to 1, and higher values mean better forecasts. For the results shown later, the TS are calculated on the 3-km SCALE model grid and with a 3-h accumulation interval, and the thresholds are chosen to be 3 mm $(3\ \mathrm{h})^{-1}$ and 15 mm $(3\ \mathrm{h})^{-1}$. We also calculate the TS with 6, 12, and 24-km grid sizes, and find that the sensitivity of TS to the grid sizes are negligible (not shown). Besides, for comparison, we conduct two other 3-km resolution SCALE forecast experiments, downscaled respectively from 1) the NCEP GFS analysis (hereafter GFS-DSCL) and 2) a 18-km SCALE-RM free-run experiment (i.e., no data assimilation) initialized from the ensemble mean analysis of the NRT SCALE-LETKF at 0000 UTC September 1, 2015, driven by the same boundary condition as in the NRT SCALE-LETKF (hereafter FR for 18-km results; FR-DSCL for 3-km results; the verification of the 18-km FR is shown in Supplement 4). More precisely, we perform 18-km resolution forecasts initialized from

the NCEP GFS analysis and FR with the NRT SCALE-LETKF domain, perform the 3-km downscaling forecasts for each, and calculate the TS accordingly. Here GFS-DSCL shows the performance of SCALE forecast using the well-established NCEP GFS initial condition, and FR/FR-DSCL represents a baseline that how worse the model forecast can be when the LETKF DA is not performed, even with the same boundary condition.

Figure 6 shows the TS of the SCALE-LETKF-DSCL, GFS-DSCL, and FR-DSCL averaged over the 3 initial times with respect to forecast hours. We find that the TS of the 48-h forecast based on the SCALE-LETKF is not significantly different from that based on the NCEP GFS analysis. In particular, GFS-DSCL shows a better precipitation forecast from 6 to 18 forecast hours, but SCALE-LETKF-DSCL outperforms, in some scores, in the first 3 hours and beyond 24 hours. The slightly better TS in the first 3 hours in SCALE-LETKF-DSCL would come from its "warm-start" type initial conditions made by a native model at native grids; whereas the NCEP GFS would reflect more accurate initial conditions, achieved by its additional satellite radiance assimilation, so that the 6−18 h TS in GFS-DSCL is better. In contrast, FR-DSCL shows almost no skill; in fact, Typhoon Etau does not exist at all in FR (not shown). Overall, in this heavy rainfall case, the NRT SCALE-LETKF system is capable of providing the initial conditions that lead to a similar forecast quality as using the operational NCEP GFS analysis, and it is much better than the free-run experiment initialized about 8 days earlier. However, we note that, for making such rainfall forecasts, running this NRT SCALE-LETKF requires more computational resources and elaborate design than directly taking the GFS analyses as initial conditions, so the practical advantages of the SCALE-LETKF need to be addressed in more careful studies, probably by assimilating higher-resolution or more frequent observation data.

5. Summary and perspectives

We developed the SCALE-LETKF system, which is a regional ensemble weather analysis and forecast system. We set up the 18-km resolution experimental NRT SCALE-LETKF for the purposes of testing its performance, stability, and feedback to the model development. The NRT cycling DA has been stably conducted for more than one year. In particular, we show the 3-km downscaling forecasts, as well as the NRT forecasts at the 18-km analysis resolution, for the September 2015 Kanto-Tohoku heavy rainfall case. The NRT SCALE-LETKF successfully analyzed the location and structure of Typhoon Etau (2015) by only the conventional observation data, and the 3-km precipitation forecasts initialized from the NRT SCALE-LETKF analysis reached a comparable skill to the same model forecast initialized from the NCEP GFS analysis.

The newly developed SCALE-LETKF provides an ensemble data assimilation package with the SCALE-RM. The SCALE-LETKF source code is available to the research community. The goal of the SCALE-LETKF is for a high-resolution, multiple-nesting regional NWP system, capable of assimilating innovative observing platforms, and this system would have a big potential for future research and applications. The use of the SCALE-LETKF system in other applications is ongoing, including the assimilation of high-density phased array weather radar data and the Himawari-8 satellite infrared radiance data.

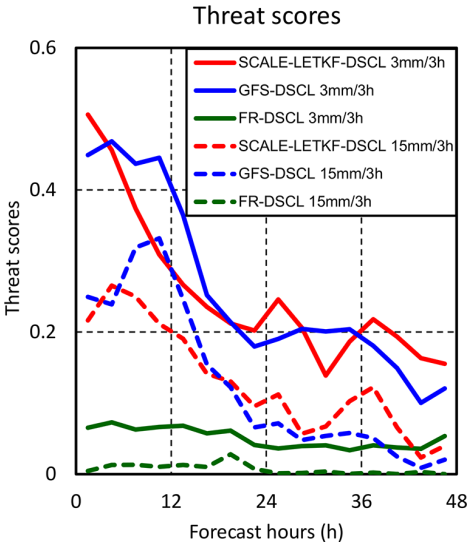

Fig. 6. The threat scores of the 3-km resolution precipitation forecasts averaged over 3 forecast initial times (12:00 UTC 8 September, 18:00 UTC 8 September, and 00:00 UTC 9 September 2015) based on (red) the SCALE-LETKF analysis, (blue) the NCEP GFS 0.5° analysis, and (green) the FR experiment. Precipitation are grouped to a 3-h accumulation interval and verified against the JMA radar based precipitation estimate. Solid and dashed lines represent the results with 3 mm (3 h)$^{-1}$ and 15 mm (3 h)$^{-1}$ thresholds, respectively.

Acknowledgements

GYL developed the SCALE-LETKF and the NRT system, performed the experiments, and analyzed the results. TM is the PI and directed the research. SN, RY, HY, SAA, TY, and HT developed the SCALE-RM model and helped substantially the development of the SCALE-LETKF. This work was supported by CREST, JST and used computational resources of the K computer provided by the RIKEN Advanced Institute for Computational Science (AICS) (Project ID: hp150019, hp160162, and ra000015). The authors thank Takumi Honda and other members of the Data Assimilation Research Team, RIKEN AICS for useful discussion. The authors also thank two anonymous reviewers for their constructive comments and suggestions.

Edited by: S.-H. Chen

Supplement

Supplement 1 lists the configurable settings in the SCALE-LETKF system.

Supplement 2 provides more verifications of the NRT SCALE-LETKF results.

Supplement 3 shows the intensity of Typhoon Etau in analyses and forecasts.

Supplement 4 shows the verification of the free-run (FR) experiment.

References

Anderson, J., T. Hoar, K. Raeder, H. Liu, N. Collins, R. Torn, and A. Avellano, 2009: The data assimilation research testbed: A community facility. *Bull. Amer. Meteor. Soc.*, **90**, 1283−1296, doi:10.1175/2009BAMS2618.1.

Beljaars, A. C. M., and A. a. M. Holtslag, 1991: Flux parameterization over land surfaces for atmospheric models. *J. Appl. Meteor.*, **30**, 327−341, doi:10.1175/1520-0450(1991)030<0327:FPOLSF>2.0.CO;2.

Bonavita, M., M. Hamrud, and L. Isaksen, 2015: EnKF and hybrid gain ensemble data assimilation. Part II: EnKF and hybrid gain results. *Mon. Wea. Rev.*, **143**, 4865−4882, doi:10.1175/MWR-D-15-0071.1.

Buehner, M., J. Morneau, and C. Charette, 2013: Four-dimensional ensemble-variational data assimilation for global deterministic weather prediction. *Nonlin. Processes Geophys.*, **20**, 669−682, doi:10.5194/npg-20-669-2013.

Evensen, G., 1994: Sequential data assimilation with a nonlinear quasi-geostrophic model using Monte Carlo methods to forecast error statistics. *J. Geophys. Res.*, **99**, 10143−10162,

doi:10.1029/94JC00572.
Evensen, G., 2003: The ensemble Kalman filter: Theoretical formulation and practical implementation. *Ocean Dynam.*, **53**, 343−367, doi:10.1007/s10236-003-0036-9.
Hunt, B. R., and co-authors, 2004: Four-dimensional ensemble Kalman filtering. *Tellus A*, **56**, 273−277, doi:10.3402/tellusa.v56i4.14424.
Hunt, B. R., E. J. Kostelich, and I. Szunyogh, 2007: Efficient data assimilation for spatiotemporal chaos: A local ensemble transform Kalman filter. *Physica D*, **230**, 112−126, doi:10.1016/j.physd.2006.11.008.
Jones, T. A., D. Stensrud, L. Wicker, P. Minnis, and R. Palikonda, 2015: Simultaneous radar and satellite data storm-scale assimilation using an ensemble Kalman filter approach for 24 May 2011. *Mon. Wea. Rev.*, **143**, 165−194, doi:10.1175/MWR-D-14-00180.1.
Kunii, M., 2014: Mesoscale data assimilation for a local severe rainfall event with the NHM–LETKF system. *Wea. Forecasting*, **29**, 1093−1105, doi:10.1175/WAF-D-13-00032.1.
Kusaka, H., H. Kondo, Y. Kikegawa, and F. Kimura, 2001: A simple single-layer urban canopy model For atmospheric models: Comparison with multi-layer and slab models. *Bound.-Layer Meteor.*, **101**, 329−358, doi:10.1023/A:1019207923078.
Mellor, G. L., and T. Yamada, 1982: Development of a turbulence closure model for geophysical fluid problems. *Rev. Geophys.*, **20**, 851−875, doi:10.1029/RG020i004p00851.
Meng, Z., and F. Zhang, 2007: Tests of an ensemble Kalman filter for mesoscale and regional-scale data assimilation. Part II: Imperfect model experiments. *Mon. Wea. Rev.*, **135**, 1403−1423, doi:10.1175/MWR3352.1.
Miyoshi, T., and K. Aranami, 2006: Applying a four-dimensional Local Ensemble Transform Kalman Filter (4D-LETKF) to the JMA Nonhydrostatic Model (NHM). *SOLA*, **2**, 128−131, doi:10.2151/sola.2006-033.
Miyoshi, T., and S. Yamane, 2007: Local ensemble transform Kalman filtering with an AGCM at a T159/L48 resolution. *Mon. Wea. Rev.*, **135**, 3841−3861, doi:10.1175/2007MWR1873.1.
Miyoshi, T., and M. Kunii, 2012: The local ensemble transform Kalman filter with the weather research and forecasting model: Experiments with real observations. *Pure Appl. Geophys.*, **169**, 321−333, doi:10.1007/s00024-011-0373-4.
Miyoshi, T., Y. Sato, and T. Kadowaki, 2010: Ensemble Kalman filter and 4D-Var intercomparison with the Japanese operational global analysis and prediction system. *Mon. Wea. Rev.*, **138**, 2846−2866, doi:10.1175/2010MWR3209.1.
Miyoshi, T., and co-authors, 2016a: "Big Data Assimilation" revolutionizing severe weather prediction. *Bull. Amer. Meteor. Soc.*, **97**, 1347−1354, doi:10.1175/BAMS-D-15-00144.1.
Miyoshi, T., and co-authors, 2016b: "Big Data Assimilation" toward post-peta-scale severe weather prediction: An overview and progress. *P. IEEE*, **104**, 2155−2179, doi:10.1109/JPROC.2016.2602560.
Nakanishi, M., and H. Niino, 2004: An improved Mellor–Yamada Level-3 model with condensation physics: Its design and verification. *Bound.-Layer Meteor.*, **112**, 1−31, doi:10.1023/B:BOUN.0000020164.04146.98.
Nishizawa, S., H. Yashiro, Y. Sato, Y. Miyamoto, and H. Tomita, 2015: Influence of grid aspect ratio on planetary boundary layer turbulence in large-eddy simulations. *Geosci. Model Dev.*, **8**, 3393−3419, doi:10.5194/gmd-8-3393-2015.
Prein, A. F., and co-authors, 2015: A review on regional convection-permitting climate modeling: Demonstrations, prospects, and challenges. *Rev. Geophys.*, **53**, 2014RG000475, doi:10.1002/2014RG000475.
Roberts, N. M., and H. W. Lean, 2008: Scale-selective verification of rainfall accumulations from high-resolution forecasts of convective events. *Mon. Wea. Rev.*, **136**, 78−97, doi:10.1175/2007MWR2123.1.
Sato, Y., S. Nishizawa, H. Yashiro, Y. Miyamoto, Y. Kajikawa, and H. Tomita, 2015: Impacts of cloud microphysics on trade wind cumulus: which cloud microphysics processes contribute to the diversity in a large eddy simulation? *Prog. Earth Planet. Sci.*, **2**, 23, doi:10.1186/s40645-015-0053-6.
Sekiguchi, M., and T. Nakajima, 2008: A k-distribution-based radiation code and its computational optimization for an atmospheric general circulation model. *Journal of Quantitative Spectroscopy and Radiative Transfer*, **109**, 2779−2793, doi:10.1016/j.jqsrt.2008.07.013.
Shao, H., and co-authors, 2015: Bridging research to operations transitions: Status and plans of Community GSI. *Bull. Amer. Meteor. Soc.*, **97**, 1427−1440, doi:10.1175/BAMS-D-13-00245.1.
Szunyogh, I., E. J. Kostelich, G. Gyarmati, E. Kalnay, B. R. Hunt, E. Ott, E. Satterfield, and J. A. Yorke, 2008: A local ensemble transform Kalman filter data assimilation system for the NCEP global model. *Tellus A*, **60**, 113−130, doi:10.3402/tellusa.v60i1.15270.
Tomita, H., 2008: New microphysical schemes with five and six categories by diagnostic generation of cloud ice. *J. Meteor. Soc. Japan*, **86A**, 121−142, doi:10.2151/jmsj.86A.121.
Torn, R. D., 2010: Performance of a mesoscale Ensemble Kalman Filter (EnKF) during the NOAA high-resolution hurricane Test. *Mon. Wea. Rev.*, **138**, 4375−4392, doi:10.1175/2010MWR3361.1.
Torn, R. D., and G. J. Hakim, 2008: Performance characteristics of a Pseudo-operational ensemble Kalman filter. *Mon. Wea. Rev.*, **136**, 3947−3963, doi:10.1175/2008MWR2443.1.
Torn, R. D., G. J. Hakim, and C. Snyder, 2006: Boundary conditions for limited-area ensemble Kalman filters. *Mon. Wea. Rev.*, **134**, 2490−2502.
Wang, X., D. Parrish, D. Kleist, and J. Whitaker, 2013: GSI 3DVar-based ensemble-variational hybrid data assimilation for NCEP global forecast system: Single-resolution experiments. *Mon. Wea. Rev.*, **141**, 4098−4117, doi:10.1175/MWR-D-12-00141.1.
Wilson, D. K., 2001: An alternative function for the wind and temperature gradients in unstable surface layers. *Bound.-Layer Meteor.*, **99**, 151−158, doi:10.1023/A:1018718707419.
Yashiro, H., K. Terasaki, T. Miyoshi, and H. Tomita, 2016: Performance evaluation of throughput-aware framework for ensemble data assimilation: The case of NICAM-LETKF. *Geosci. Model Dev.*, **9**, 2293−2300, doi:10.5194/gmd-9-2293-2016.
Yussouf, N., E. R. Mansell, L. J. Wicker, D. M. Wheatley, and D. J. Stensrud, 2013: The ensemble Kalman filter analyses and forecasts of the 8 May 2003 Oklahoma City tornadic supercell storm using single- and double-Moment microphysics schemes. *Mon. Wea. Rev.*, **141**, 3388−3412, doi:10.1175/MWR-D-12-00237.1.
Zhang, F., and Y. Weng, 2015: Predicting hurricane intensity and associated hazards: A five-year real-time forecast experiment with assimilation of airborne Doppler radar observations. *Bull. Amer. Meteor. Soc.*, **96**, 25−33, doi:10.1175/BAMS-D-13-00231.1.
Zhang, F., C. Snyder, and J. Sun, 2004: Impacts of initial estimate and observation availability on convective-scale data assimilation with an ensemble Kalman filter. *Mon. Wea. Rev.*, **132**, 1238−1253, doi:10.1175/1520-0493(2004)132<1238:IOIEAO>2.0.CO;2.
Zhang, F., Z. Meng, and A. Aksoy, 2006: Tests of an ensemble Kalman filter for mesoscale and regional-scale data assimilation. Part I: Perfect model experiments. *Mon. Wea. Rev.*, **134**, 722−736.
Zhang, F., Y. Weng, J. A. Sippel, Z. Meng, and C. H. Bishop, 2009: Cloud-resolving hurricane initialization and prediction through assimilation of Doppler radar observations with an ensemble Kalman filter. *Mon. Wea. Rev.*, **137**, 2105−2125, doi:10.1175/2009MWR2645.1.

Manuscript received 7 July 2016, accepted 28 November 2016
SOLA: https://www.jstage.jst.go.jp/browse/sola/